LBNL-54097

CHARACTERIZATION OF HIGH-POWER LITHIUM-ION CELLS-PERFORMANCE AND DIAGNOSTIC ANALYSIS

K.A. Striebel[a], J. Shim[a], R. Kostecki[a], T.J. Richardson[a], P.N. Ross[b], X. Song[a], G. V. Zhuang[b]

[a]Environmental Energy Technologies Division
[b]Materials Science Division
E.O. Lawrence Berkeley National Laboratory
Berkeley, CA 94720 USA

ABSTRACT

Lithium-ion cells, with graphite anodes and $LiNi_{0.8}Co_{0.15}Al_{0.05}O_2$ cathodes, were cycled for up to 1000 cycles over different ranges of SOC and temperatures. The decline in cell performance increases with the span of SOC and temperature during cycling. Capacity fade was caused by a combination of the loss of cycleable Li and degradation of the cathode. The room temperature anodes showed SEI compositions and degrees of graphite disorder that correlated with the extent of the Li consumption, which was linear in cell test time. TEM of the cathodes showed evidence of crystalline defects, though no major new phases were identified, consistent with XRD. No evidence of polymeric deposits on the cathode particles (FTIR) was detected although both Raman and TEM showed evidence of P-containing deposits from electrolyte salt degradation. Raman microscopy showed differences in relative carbon contents of the cycled cathodes, which is blamed for part of the cathode degradation.

INTRODUCTION

Lithium ion batteries are being seriously considered for application in all-electric vehicles (EV) and hybrid electric vehicles (HEV's) because of their high power and energy densities [1-2]. The cathode active material, $LiNi_{0.8}Co_{0.15}Al_{0.05}O_2$, was chosen for the cathode-active material in a large study by the DOE Advanced Technology Development (ATD) project, as their Generation 2 cell chemistry, together with an anode based on Hitachi's Mag-10 graphite. The ATD program has been directed at the understanding of this cell chemistry during in calendar life studies and pulsed-lifecycle testing over a very limited range of state-of-charge (SOC) [3], as required by the HEV application. Many cells have been examined to determine the mechanisms for capacity and power fade, with a wide range of diagnostic techniques, developed and refined during studies of the ATD Gen 1 cells [4,5].

In the parallel DOE project, the Batteries for Advanced Transportation Technologies (BATT) program, research is aimed at batteries for the EV application, as well as for HEV. To benchmark the $LiNi_{0.8}Co_{0.15}Al_{0.05}O_2$/Mag-10 cell for the EV application, we prepared and studied 12 cm^2 pouch cells, with a chemistry very similar to that in the ATD Gen 2 18650 cells and cycled them over either 70 or 100% depth-of-discharge (DOD) at room temperature or 60°C. The cycle performance for these cells has been reported

previously [7,8]. With a wider swing in SOC during cycling, these cells were seen to loose power and capacity at a much faster rate than the ATD cells. In this paper, the results of several diagnostic analyses of the cell components are presented in an effort to understand the influence of the cycling profile on component degradation.

EXPERIMENTAL

The pouch cells were constructed from Quallion Corps electrodes containing Hitachi Mag-10 graphite and Fuji $LiNi_{0.8}Co_{0.15}Al_{0.05}O_2$ active materials and LP40 electrolyte (1M $LiPF_6$ in 1:1 EC/DEC) from EM Science. Details of the cell construction were reported previously [7]. After formation, cycle-life testing was carried out at C/2 with discharges to either 3.0V (100% DOD) or to a capacity limit of 0.7C (70% DOD). Cycling was interrupted every 80 cycles to measure cell impedance and pulse power capability with the Hybrid Pulse Power Characterization (HPPC) profile [6]. One cell was cycled at 60°C with the remainder cycled at room temperature. At the end of cycling, the cells were again subjected to a C/25 cycle, ending at 3.0V(100%DOD) to determine the capacity remaining in the cell. The discharged cells were disassembled in an Ar glovebox. Electrodes were soaked in DEC overnight and dried in the glovebox prior to sampling for the various diagnostic techniques.

An integrated Raman microscope system "Labram" made by ISA Groupe Horiba was used to analyze the structure and composition of the cathodes and anodes. The FTIR measurements were performed on a Nicolet Nexus 870 Spectrometer, equipped with a broadband Mercury-Cadmium-Telluride (MCT) detector. The spectra were acquired in the Attenuated Total Reflection (ATR) mode using a hemispherical Ge optic at a spectral resolution of 4 cm^{-1}. For TEM measurements, samples were dispersed on a copper grid and studied in a Philips CM200/FEG (field emission gun) TEM at the National Center for Electron Microscopy (NCEM) at LBNL.

RESULTS AND DISCUSSION

The C/2 discharge capacities for the cells in this study are shown in Figure 1. The cycling conditions and measures of performance fade are summarized in Table 1. Low-rate capacity measurements were made before cycling (the second formation cycle) and after cycling was completed. The capacity fade during C/2 cycling is larger than the low-rate (C/25) fade since the impedance of the cell is also increasing. From these data it is clear that the capacity of cells cycled over 100% DOD and at high-temperature fades faster than that of cells cycled at room temperature and/or a more limited capacity range. The capacity fade in the 70%DOD cell was estimated by comparison of the end-of-discharge voltage, which dropped from 3.55 to 3.4V over 1000 cycles, with the original C/25 discharge curve.

For comparison of these results with those from the ADT cells undergoing life-cycle testing with the 25kW Power Assist Life Cycle (PALC) profile, developed by PNGV [6],. we need to estimate the equivalent charge passed during a week. We calculated an equivalent of about 77 PALC cycles per 100% DOD cycle, or 435 full 100% DOD cycles per 4-week test period in the ATD program. The ATD cells showed an equivalent of 6% capacity fade (at C/25) at this time in their life [21]. This can be compared with 11% capacity fade for 1000 cycles at 70% DOD and 14% for 480 cycles at 100% DOD cycling in our cells, suggesting a direct correlation between SOC-swing (or lower voltage

limit) during cycling and capacity fade.[10]. The rate of cell impedance rise on cycling method can also be compared. The 4 wk ATD cells showed an impedance rise of only 4% [21], while the pouch cells in this study showed impedance rises of 10% and 35% for the 70%DOD-1000 and 100%DOD-480 cycled cells, respectively.

To understand the reasons for the affect of cycling regime on performance fade, cells were disassembled after a C/25 discharge for electrochemical, chemical and physical diagnostics. Electrochemical diagnostic studies of each electrode were carried out in half-cells, as discussed previously [7,8]. The capacity of the anodes from the 25°C-cycled cells, showed essentially identical capacity to the fresh anodes in half-cell measurements. The anode cycled at 60°C showed a capacity loss of only 10%. The electrochemical diagnostics on the cathodes removed from the cycled cells (Figure 2) shows the C/25 cycles of the cathode removed from the cell cycled at 1000 times over 100%DOD. The first charge for the cathode post-test reveals the amount of cycleable lithium remaining in the cell. The difference between the original Li content and that remaining in the cell will be equal the loss of Li during cycling, after correction for the first cycle inefficiencies in the electrodes, due to a combination of side-reaction, isolation within the cathode or conversion to a non-active phase. Comparison between the second post-test cycle on the cathode with the same test on fresh (uncycled) cathode reveals the decline in the ability of the electrode to intercalate lithium, given a fresh (and large) source of lithium. The amount of lithium consumed in this reaction is shown in Figure 3, to correlate with the total test time for the cell.

The ATD program has observed two regimes of performance fade with different time-dependencies. The first period non-linear of power fade, lasting on the order of 30-40 weeks, has been attributed to changes in the cathode. After this period, the behavior of the anode starts to limit the performance as a linear function of time [21]. In this work, we have many fewer cells to examine and cannot form such an extensive picture of the time dependence of the performance decline. However, within the 11 weeks of these pouch cell tests, the anodes in all of these cells showed very little change in electrochemical performance when matched against a large source of cycleable Li. In addition, the consumption of the cycleable Li is a linear process in time and the impedance growth of the SEI might be expected also to grow linearly, consistent with the ATD results.

Diagnostics Analysis of the Cathode

XRD patterns for cathode samples removed from these cells showed any evidence of new phases that could be held responsible for some of the degradation, even for the cell cycled at 60°C [10].

A typical infrared spectrum from the PG03 cathode is shown in Fig.4. The FTIR spectra from all four cells were essentially identical (the backgrounds were different due to differences in surface morphology). Although weak peaks characteristic of the carbonyl group in EC (at 1804 cm^{-1} and 1774cm^{-1}) were still discernable, features in the spectral regions between 1300 cm^{-1}– 700 cm^{-1} are the most prominent and are not solvent or electrolyte related. Most of these features could be readily assigned to PVDF, as shown by comparison with the reference spectrum from a PVDF powder (Fig. 4a). Interestingly, the spectral difference in the 1600 cm^{-1} to 1300 cm^{-1} region between that from the virgin cathode (before assembly into a cell) and that after cycling in the cell was quite striking. The strong peak at 1416 cm^{-1} and a shoulder at 1500 cm^{-1} are the C-O

asymmetric and symmetric stretching modes of Li_2CO_3. Interestingly, no residual lithium carbonate was detected in the spectra of any of the cathodes of cycled cells, as clearly indicated by the absence of the strong peak at 1422 cm^{-1} and its shoulder at 1493 cm^{-1}. The fate of the Li_2CO_3 during the cycling is still unknown. Furthermore, there is no evidence of any insoluble (in DEC) film on the cathode produced by reaction with the electrolyte.

Raman microprobe spectra taken from different locations on the cathodes varied strongly between different grains suggesting the presence of delithiated $Li_{1-x}Ni_{0.8}Co_{0.15}Al_{0.05}O_2$ phases in close proximity to fully lithiated material in the tested cathodes despite the cathodes being slowly discharged before sampling [10]. The cathodes from the room temperature cells exhibited a mixture of fully discharged and partially charged particles of $Li_{1-x}Ni_{0.8}Co_{0.15}Al_{0.05}O_2$ at the surface while, the surface of the 60°C-cycled cathode consisted of fully charged active material. Cathode surface average composition maps, also produced with the Raman microscope (not shown), indicated that active material/carbon surface concentration ratios were higher for the cells with higher cathode capacity fade. Previous results for the cathode cycled at 60°C showed a complete lack of conductivity of the cathode surface [7] consistent with either loss of contact of particles at the electrode surface with the rest of the electrode, or the presence of a non-conductive film. A reduction in the conductive nature of portions of the electrode can easily explain rises in the cell impedance as well as losses in capacity through isolation of active material.

TEM observations, carried out with cathode samples from the room-temperature-cycled cathodes, showed evidence of a layer of about 5 nm thick on the surface of a $LiNi_{0.8}Co_{0.15}Al_{0.05}O_2$ grain from the PG03 cathode (see Fig. 5). An EDX spectrum (not shown) showed no metallic impurities, but did show traces of P, from degradation products from the electrolyte salt, consistent with the results from the Raman spectroscopy. From the FTIR results, this is not an organic layer, and it is not a carbonate layer, which is clearly removed with cycling by this time. However, FTIR will not distinguish a LiF layer or an oxide layer, such as Li_2O. In addition, many defects, stresses, and dislocations were directly observed in the $LiNi_{0.8}Co_{0.15}Al_{0.05}O_2$ grains [10]. For all of these techniques, the cathodes were analyzed after washing in DEC. It is quite possible that there was some sort of soluble organic layer on the cathode that was removed during washing that is responsible for additional surface impedance.

Diagnostic Analysis of the Anode

Raman spectroscopy is a particularly useful tool for characterizing the near-surface structure of graphite because of its relatively large Raman scattering cross-section. A typical Raman spectrum of graphite consists of two E_{2g} active modes: a strong (G) band at ~1582 cm^{-1} and a weak band at 42 cm^{-1}, which is difficult to observe. However, decreasing intra-planar (L_a) and inter-planar (L_c) graphite microcrystalline dimensions always give rise to a new feature at ~1360 cm^{-1}. This (D) band, which is assigned to the A_{1g} mode, is associated with the breakage of symmetry occurring at the edges of graphite sheets. The relative intensity of the D band *vs*. G band is attributed to increased carbon disorder [15,16]. The D/G band was calculated for a freshly-formed MAG-10 graphite anode and the anodes from the cycled cells. This ratio is plotted along with the loss of cycleable Li against test time in Fig. 3. Except for the anode cycled at

60°C, which showed a huge increase of the D/G ratio and broadening of the G band, in a very short cycling time, the D/G intensity ratios correlate reasonably well with test time.

FTIR spectra (not shown) obtained from the anodes were qualitatively similar, but quantitatively different. Specifically, the relative ratio of features between 1700-1550 cm^{-1} (organic components) and those between 1550-1140 cm^{-1} (inorganic components) vary significantly among these cells. However, the overall spectral features from different cells could be fit with the same mixture of lithium compounds. They were all simulated by the superposition of individual spectra for lithium carbonate (Li_2CO_3), lithium formate (LiOOCH), lithium succinate ($LiO_2CCH_2CH_2CO_2Li$), and lithium methoxide ($LiOCH_3$). The anode from the cell cycled at high temperature, had a uniquely different spectrum from the room temperature cycled cells, having the most carbonate (Li_2CO_3) and least carboxylate content [10]. The ratio of the inorganic fraction of the SEI layer to that of the organic component (I/O) for each anode is also plotted in Fig. 3. It appears that there is either an increase in the inorganic component or a conversion from organic to inorganic with test time.

Peled et al. [22] found that inorganic products dominate the SEI on the graphitic plane cross-section whereas a thin layer of organic polymers covers the basal planes. Kostecki and McLarnon found that the SEI layer on graphite electrodes changes in both morphology and chemical composition due to gradual structural degradation of the graphite upon electrochemical cycling [16]. The correlation between conversion of organic SEI to inorganic SEI and the increasing disorder in the anode graphite and various measures of capacity and power fade in the cells, suggested in Fig. 3, is consistent with these observations, at least for the room temperature cells. It is probable that further conversion in the surface chemistry will take place at longer times and higher temperatures. The high temperature cell showed only a relatively small amount of Li consumption in the short test time, with a mostly inorganic SEI, suggesting that another degradation mechanism may be operative at this temperature, such as the production of LiF type components or an increase in the depth of the disorder due to increased solvent intercalation.

CONCLUSIONS

Cycling regime was found to have a large impact on the capacity and power fade mechanisms occurring in $LiNi_{0.8}Co_{0.15}Al_{0.05}O_2$/graphite pouch cells. From a comparison of cells cycled over 100% and 70% DOD with the ATD cell (cycled at ± 5% DOD), the performance decline was found to increase with the span of the DOD during cycling. The loss of cycleable Li, most likely due to solvent reduction on the anode, was found to be linear in cell test time. In addition, the room temperature cells showed an SEI composition (inorganic vs organic fraction) and degree of graphite disorder on the anode surface, which roughly correlated with each other and with the extent of the Li consumption.

Post-test electrochemical analysis of the anode and cathode revealed changes in the anode SEI but that cathode degradation is most significant to cell performance fade. TEM showed evidence of and SEI layer and crystalline defects though no major new phases were identified, in agreement with the XRD results. Neither FTIR or Raman analysis of the cathode revealed evidence of polymeric deposits on the cathode although both Raman and TEM showed evidence of P-containing deposits from electrolyte salt degradation. A noticeable difference in the active material to carbon surface concentration ratio for the cycled cathodes that was observed by Raman mapping. The origin of this effect is still

unknown and more work is clearly needed to understand exactly its mechanism and possible implications on the cathode electrochemical properties.

ACKNOWLEDGEMENTS

This research was funded by the Assistant Secretary for Energy Efficiency and Renewable Energy, Office of Advanced Automotive Technologies, U. S. Department of Energy, under contract number DE- AC03-76SF00098.

REFERENCES

1. G. Nagasubramanian, R.G. Jungst, D.H. Doughty, *J. Power Sources*, **83**, (1999) 193
2. Q. Wu, W. Lu, J. Prakash, *J. Power Sources*, **88** (2000) 237.
3. Raymond A. Sutula et al., "FY 2001 Progress Report for the Advanced Technology Development Program," U.S. DOE OAAT, February 2001.
4. X. Zhang, P.N. Ross, R. Kostecki, F. Kong, S. Sloop, J.B. Kerr, K.A. Striebel, E.J. Cairns, F. McLarnon, *J. Electrochem. Soc*., **148,** A463 (2001).
5. "Advanced Technology Development Program for Lithium-Ion Batteries: Handbook of Diagnostic Techniques," G.Henriksen, J. McBreen and F. McLarnon, eds., Lawrence Berkeley National Laboratory Report No. LBID-2464, Berkeley, CA., April 2003.
6. T.Q. Duong, *J. Power Sources,* **89**, 244 (2000).
7. J. Shim, R. Kostecki, T. Richardson, X. Song, K.A. Striebel, *J. Power Sources*, **112** 222, (2002).
8. J. Shim and K. Striebel, *J. Power Sources*, in-press, 2003.
9. Jon P. Christophersen et al., "Advanced Technology Development For Lithium-Ion Batteries: Gen 2 Performance Evaluation Interim Report," INEEL/EXT-03-00095, February 2003. 21
10. K.A. Striebel, J. Shim, E.J. Cairns, R. Kostecki, Y.-J. Lee, J. Reimer, T.J. Richardson, P.N. Ross, X. Song, G. V. Zhuang, J. Electrochem. Soc., submitted, 2003.
11. R. Vidano, D.B. Fischbach, *J. Amer. Ceramic Soc.,* **61,** 13, (1978).15
12. R. Kostecki and F. McLarnon*, J. Power Sources*, **119-121**, 550, 2003, 16
13. E. Peled, D. Bar Tow, A. Merson, A. Gladkich, L. Burstein, D. Golodnitsky, *J.Power Sources,* **97/98,** 52, (2001). 22

Table 1. Cell Performance

Cell Name	DOD (%)	Temp. (°C)	# Cycles	Cell Power Fade	Cell ASI @ EOD	Capacity Fade			
						Cell, C/2	Cell C/25	Pos. C/25	Neg. C/25
PG13	100	60	140	NA	+32%	65%	39%	59%	10%
PG04	100	25	480	70%	+35%	30%	14%	18%	0%
PG03	100	25	1000	NA	+78%	70%	40%	27%	0%
PG06	70	25	1000	45%	+10%	14%*	11%	5%	0%

*from the 100%DOD C/2 cycle in the final RPT, the cell delivered of 70% capacity throughout 1000 cycles

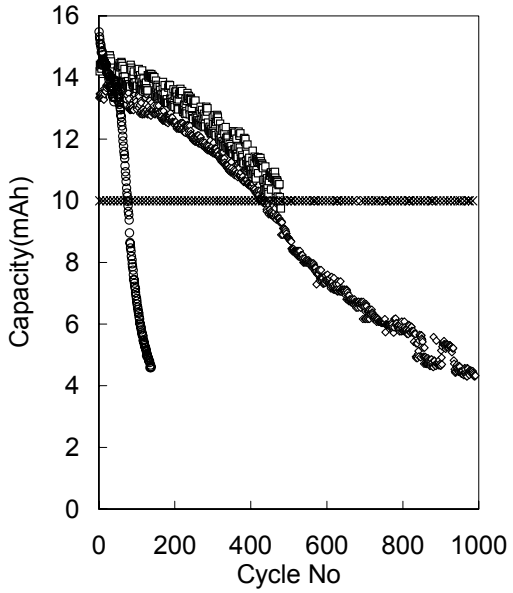

Figure 1. Discharge capacity of 12 cm^2 $LiNi_{0.8}Co_{0.15}Al_{0.05}O_2$/Mag-10 pouch cells: 100%DOD: ◊ PG03, PG04, 70%DOD: × PG06, and 100%DOD at 60°C: o PG13

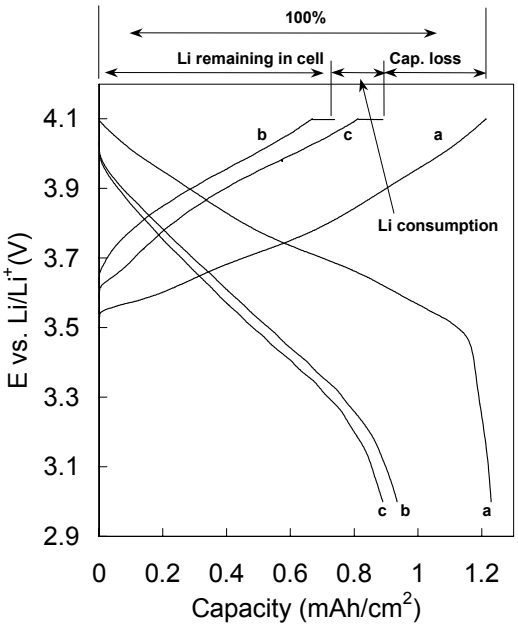

Figure 2. Electrochemical diagnostics of a cathode vs. Li, removed from the PG03 cell (a) fresh cathode,(b) first post-test cycle, and (c) second post-test cycle.

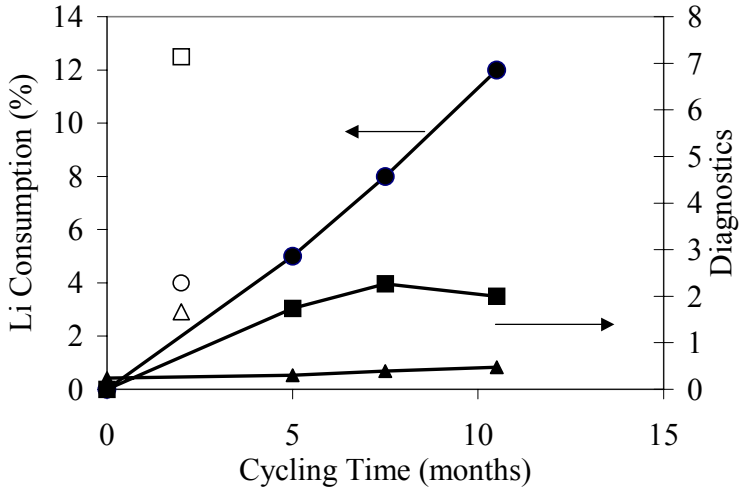

.

Figure 3. Diagnostic parameters shown as a function of time, room temperature cells (closed symbols) and 60°C cell (open symbols): Li consumption calculated as shown in Fig. 2 (●, o); I/O ratio from FTIR data (■,), D/G ratio from Raman data (▲, △).

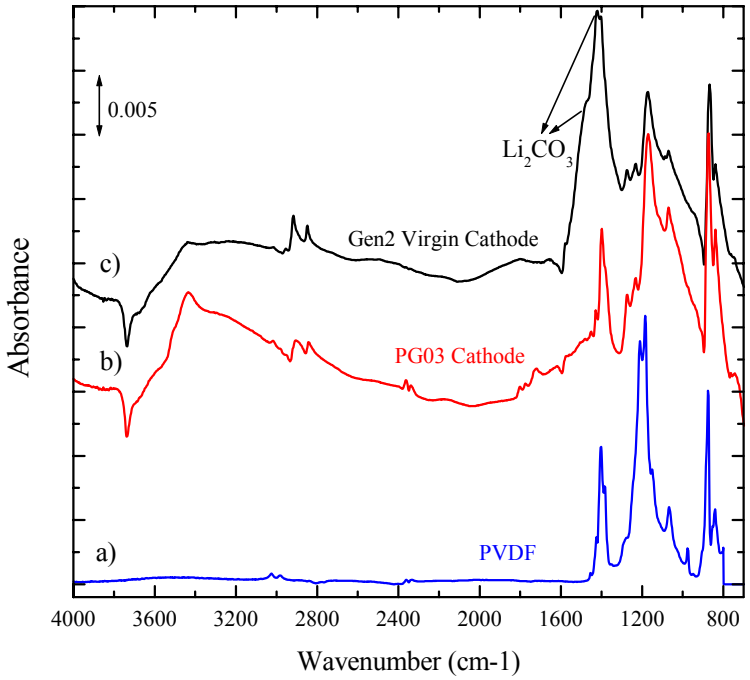

Figure 4. FTIR-ATR spectra for two cathodes and pure PVdF.

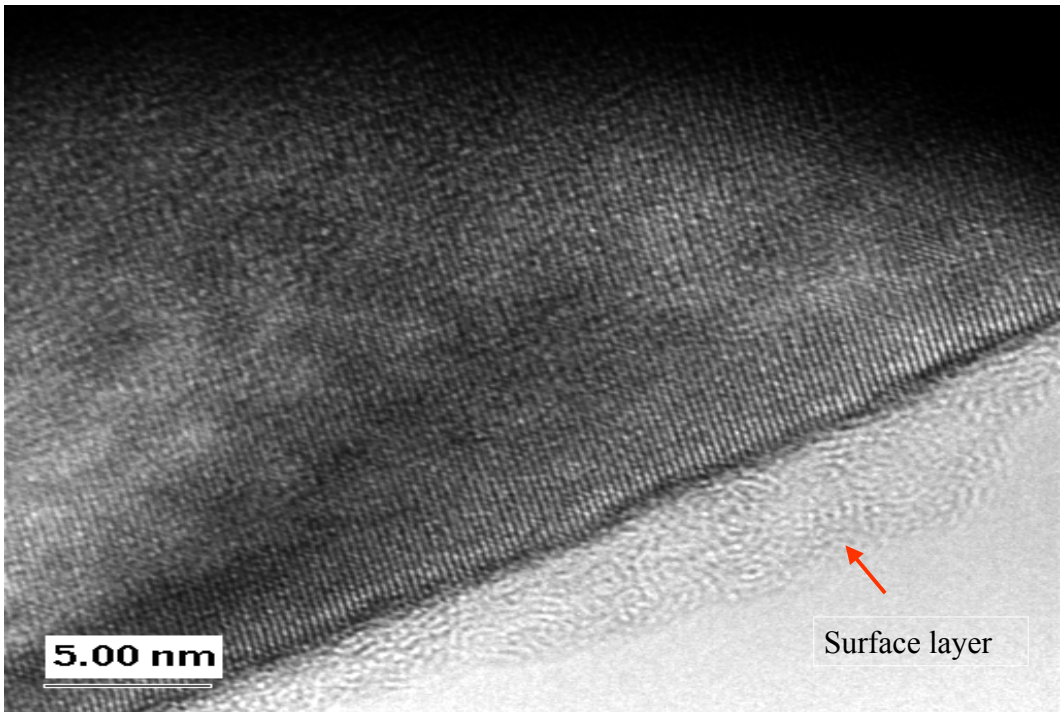

Figure 5. Lattice image of a $LiNi_{0.8}Co_{0.15}Al_{0.05}O_2$ grain with the SEI layer labeled by an arrow.

Key words: Lithium ion battery, diagnostics, Raman, FTIR, TEM